Intermolecular HH Vibrations of Dihydrogen Bonded Complexes $H_3EH^-\cdots HOR$ in the Low-Frequency Region: Theory and IR Spectra

Oleg A. Filippov,[†,‡] Victoria N. Tsupreva,[†] Lina M. Epstein,[†] Agusti Lledos,*[,‡] and Elena S. Shubina*[,†]

A.N. Nesmeyanov Institute of Organoelement Compounds, Russian Academy of Sciences, Vavilov Street 28, 119991 Moscow, Russia, and Departament de Química, Edifici Cn, Universitat Autónoma de Barcelona, 08193 Bellaterra, Spain

Received: May 15, 2008; Revised Manuscript Received: June 23, 2008

The results of DFT calculations of harmonic and anharmonic frequencies of the dihydrogen bonded (DHB) complexes $H_3EH^-\cdots HOR$ (E = B, Al, Ga and HOR = CH_3OH, CF_3CH_2OH) in gas phase and in low polar medium (by CPCM model) in comparison with the partners are presented. Normal coordinate analysis of the low-frequency modes was carried out to assign the new vibrations induced by DHB formation by the potential energy distribution values. Among them, the intermolecular H···H stretching vibrations only have individual modes. The influence of central atom mass and isotope and the strength of the proton donor effects were determined. The systems convenient for IR studies were chosen from the calculation predictions. The spectral investigation was made on the BH_4^-/ROH complexes (ROH = CH_2FCH_2OH (MFE), CF_3CH_2OH (TFE), $(CF_3)_2CHOH$ (HFIP)). The results of temperature dependence, isotope substitution, and influence of the proton-donor strength studies agree with the theoretical conclusions. Combination of experimental and theoretical approaches allowed determining for the first time the intermolecular stretching mode characterizing intrinsic DHB vibrations.

1. Introduction

A new type of hydrogen bond (HB), the so-called dihydrogen bond (DHB), was discovered and intensively investigated over the past decade.[1−6] In these HB which have no analogues in organic chemistry, the proton-accepting site is a hydrogen atom of transition metal or main-group hydride complexes. The interest in XH···HE (E = transition metal or main-group element) DHB complexes increases because of the possibility they offer of controlling reaction stereoselectivity and directing the organization of H···H-based supramolecular structures.[7−20] The experimental methods for DHB investigations are IR, NMR, UV−vis, and X-ray as in the case of classical HBs. Yet, a lot of papers have been devoted to theoretical investigations of structure and energy of DHB complexes, including frequency calculations.[21−28] Thus, the intermolecular stretch EH···HX, which is of special interest in this paper, was reported for DHB complexes MoH···HOR,[21] BeH···HCN,[28] MH···HX (M = Na, Li; X = F, Cl, Br),[29] MH···HC (M = Zn, Cd),[30] and AlH···HRgF (Rg = Ar, Kr).[31] However, the bands assignment was made without normal coordinate analysis, which should include potential energy distribution (PED) calculations and, strictly speaking, is a prerequisite for such type of research. Recently, by studying the proton transfer and H_2 elimination reaction between main-group hydrides and alcohols EH_4^-/HOR (E = B, Ga, Al) by combining theoretical calculations and spectroscopic studies of OH and EH stretching vibrations, we provided the analysis of the structure and thermodynamic characteristics of DHB complexes formed at the first step of this reaction.[12−14] Here, we present the results of a combined computational and experimental study of a series of EH_4^-/HOR DHB complexes aimed to assign the low-frequency modes, in particular those induced by DHB formation, determine individual/mixing modes by PED, and identify the intermolecular H···H stretching vibration. DFT calculations of the harmonic vibrational frequencies of EH_4^-/HOR DHB complexes were carried out both in gas phase and in a low polar media (CH_2Cl_2). Anharmonicity effects were also considered, and normal coordinate analysis was also performed. Then, following the theoretical predictions, IR spectral investigation of the BH_4^-/ROH complexes (ROH = CH_2FCH_2OH (MFE), CF_3CH_2OH (TFE), $(CF_3)_2CHOH$ (HFIP)) was pursued to find out the intermolecular stretching vibration and to characterize the spectral properties of DHB formation in the low-frequency range.

2. Experimental and Computational Methods

2.1. Experimental Details. As hydride complex, the commercially available salt Bu_4NBH_4 (Sigma) was used. The fluorinated alcohols FCH_2CH_2OH, CF_3CH_2OH and $(CF_3)_2$-CHOH (P&M, Moscow) were used as proton donors. Solvents (CH_2Cl_2 and $(CH_2Cl)_2$) were dried by reflux over CaH_2 in the Ar atmosphere prior to use.

IR measurements were carried out on a Specord M82 (Carl Zeiss Jena) spectrometer and Magna-IR-750 (Nicolet) FTIR spectrometer. For the low-temperature measurements, a cryostat Carl Zeiss Jena was employed in the temperature range 190−300K by using a stream of liquid nitrogen. The accuracy of temperature adjustment was ±0.5 °C. The reagents were mixed at low temperatures to prevent the dihydrogen evolution, and the cold solution was transferred into the cryostat pre-cooled to a required temperature. The measurements in the low

* Corresponding author. (E.S.S) Tel: +7(499)1351871. Fax +7(499)1355085. E-mail: shu@ineos.ac.ru. (A.L.) Tel: +34(93)5811716. Fax:+34(93)5812920. E-mail: agusti@klingon.uab.es.
† Russian Academy of Sciences.
‡ Universitat Autónoma de Barcelona.

10.1021/jp804303j CCC: $40.75
Published on Web 08/13/2008

frequency range (300−600 cm^{-1}) were made in polyethylene cells ($d = 0.12$ cm). Unfortunately, it was impossible to provide the measurements in the range lower than 300 cm^{-1} because the strong bands of the media used. Use of other solvent is restricted by insolubility of the salt in aromatic and linear hydrocarbon low polar solvents and interaction with CH_3I. The concentrations of proton donors were between 10^{-2} and 10^{-3} mol/L, and IR spectra were measured in excess of boron tetrahydride ($c = 10^{-1}-10^{-2}$ mol/L). Anhydrous solvents were freshly distilled and degassed prior to use.

2.2. Computational Details. The geometries of DHB complexes EH_4^-/ROH (E = B, Al, Ga; ROH = CH_3OH, CF_3CH_2OH, $(CF_3)_2CHOH$) were optimized with Gaussian03[32] by DFT/B3LYP[33] and MP2[34] methods employing the 6-311++G (d,p) basis set, which have been shown to yield accurate optimized structures of the complexes.[14] In order to obtain precise force constant matrix, DHB complexes and monomers were additionally optimized by implying tight optimization criteria (OPT=VERYTIGHT) with ultra fine grid (GRID=ULTRAFINE). For taking into account the nonspecific solvent effect, geometry optimizations in dichloromethane (DCM, $\varepsilon = 8.93$) were carried out by using the CPCM continuum representation of the solvent.[35] Frequency calculations were performed both in the gas phase and in DCM solvent by using the corresponding optimized structures. In vacuum, anharmonic frequency calculations were done by using a second-order perturbative treatment implemented in the Gaussian 03 package.[36,37]

The normal coordinate analysis and PED calculations were performed for all gas-phase optimized DHB complexes with the program DISP[38] by using equilibrium geometries and Cartesian force constants from Gaussian output files. DISP was used for transformation of the equilibrium geometries and the Cartesian force constants into the redundant internal coordinates and force constants with minimal off diagonal terms. PED was expressed as relative contribution of each internal coordinate to the potential energy of the given normal vibration. The predominant vibrational motion determined by the PED analysis was used to name each fundamental mode for all the free monomers and DHB complexes.

3. Results and Discussion

3.1. Theoretical Study of the Vibration Spectra. The complete assignment of the vibrational spectra for DHB complexes was made on the basis of the normal-mode analysis (including PED) for DHB complexes in comparison with those of the free partners. The assignment of the vibrations with a high degree of mixing of the different normal modes was further checked by considering the complexes with alcohol of increasing acidic strength and confirmed by the experimental study (see below). Calculations were carried out both in the gas phase and in low polar media (CH_2Cl_2). The results of harmonic and anharmonic frequency calculations were also compared.

Because the theoretical EH stretching vibrations in DHB complexes were presented in our previous paper,[14] herein, we concentrate on the analysis of the low-frequency vibrations (0−720 cm^{-1}). The comparison of the effects of dihydrogen bonding formation in low frequencies with those in OH stretching vibrations will be presented at the end of the spectral part from the standpoint of the complex strength and structure.

Isolated EH_4^- hydride anions have no vibrations in the low-frequency range, whereas CH_3OH exhibits one highly characteristic band τ(OH) at 303 cm^{-1}. Upon DHB complex formation, τ(OH) shifts to the 700 cm^{-1} range (ν_7 in Table 1), and six new vibrations appear in this region (Table 1, $\nu_1-\nu_6$). Three of them are mixed torsion vibrations ($\tau(CH_3OH)$, $t(CH_3)$, (tEH_3)), and two are deformations of the H-bond (δ(OH···H), δ(EH···H)). The frequencies of the last ν_5 vibration are practically similar for all central elements (137−142 cm^{-1}) and possess individual mode δ(EHH) (PED = 86−99%). The following ν_6 vibration is the intermolecular highly characteristic H···H stretch named ν_σ (Table 1). The maximal individuality of this mode is found for DHB of BH_4^- (PED = 102%), and to a lesser degree, it is characteristic for complexes with Al and Ga hydrides (81% for both complexes). The frequencies of this mode are located in the range lower than 400 cm^{-1} and dramatically decrease when going from BH_4^-/CH_3OH to the corresponding DHB of AlH_4^- ($\Delta\nu = 61$ cm^{-1} for DHB with CH_3OH). Notably, the further step to gallium analogue does not practically change this frequency and PED (Table 1).

For comparative purposes, the theoretical analysis of TFE (Table 2) and its complexes with EH_4^- hydrides (Table 3) was carried by using both B3LYP and MP2 calculations. In addition, anharmonicity corrections were introduced in the B3LYP calculations. Calculations of more complex alcohol CF_3CH_2OH (TFE) show seven vibrations in the low-frequency range (0−600 cm^{-1}, Table 2). The assignment of TFE frequencies is clear because of PED values. The lowest two bands are assigned to the modes of t C-CH_2, mixed δCF_3 and δOCC; frequencies **3** and **4** belong to the mixed torsion OH and deformation CF_3 modes. The three higher frequencies, **5**−**7**, involve 50−73% of the CF_3 groups deformations. The differences between the values of the harmonic MP2 and B3LYP frequencies are small (9−18 cm^{-1}), and they are between harmonic and anharmonic B3LYP frequencies (1−10 cm^{-1}) with the exception of **3** and **4** vibrations. Anharmonicity has profound effect ($\Delta\nu = 23-26$ cm^{-1}) on these frequencies because of the great impact of τOH mode. Harmonic MP2 frequencies are always slightly higher than the corresponding B3LYP ones, in agreement with the derived scale factors for both methods.[39,40]

DHB complexes possess in this range 12 vibrations. As for free TFE, the MP2 harmonic frequencies are also a little higher (1−17 cm^{-1}) than these calculated by B3LYP with only one exception with δBH···H mode, **6** ($\Delta\nu = 23$ cm^{-1}).[39,40] Although in general, anharmonicity has less effect ($\Delta\nu = 1-9$ cm^{-1}) than the method of calculation, anharmonicity manifests a significant influence on the frequencies for the mixed vibrations with a great impact of δOH···H modes (**3**, **5**) and for the two characteristic ones, **6** (δBH···H) and **8** (ν_σ). These frequencies decrease on 25−28 cm^{-1} under this effect. Complexation with the hydride leads to a very little shift of the three higher bands (**9**−**12**) ($\Delta\nu = 2-4$ cm^{-1}, compare Tables 2 and **3**) with preservation of their modes (δCF_3). Significant changes appear in the range 300−400 cm^{-1}. Instead of the two free TFE frequencies **3** at 315 (harmonic) and 292 cm^{-1} (anharmonic) and **4** at 382, 356 cm^{-1} (Table 2), the frequencies of DHB complexes appear, **8** at 338, 310 cm^{-1} and **9** at 349, 345 cm^{-1} (Table 3). The calculations indicate transformation of the modes during DHB formation from mixed torsion and bending (**3** and **4**, Table 2) into bending $\delta(CF_3)$ (**9**, Table 3) with significant increase of the torsion τOH mode frequency to 709 cm^{-1} as well as appearance of the new H···H stretching mode **8** (harmonic 338, anharmonic 310 cm^{-1}). On the whole, the calculations present the assignment in the low-frequency range of DHB complexes with two proton donors (CH_3OH and CF_3CH_2OH), allowing us to consider the influence of the computation level and properties of the partners on the frequencies and modes.

TABLE 1: Calculated B3LYP Gas-Phase Harmonic Frequencies of EH_4^-/CH_3OH Dihydrogen-Bonded Complexes in the Low-Frequency Range and their Assignment According to the PED Values[a]

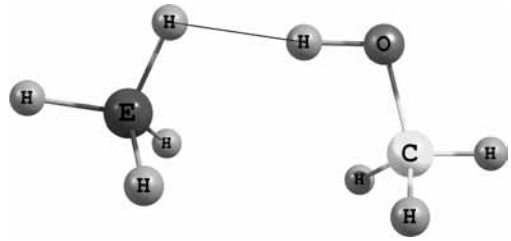

BH_4^-			GaH_4^-			AlH_4^-		
ν, cm^{-1}	mode	PED	ν, cm^{-1}	mode	PED	ν, cm^{-1}	mode	PED
				ν_1				
55	τCH_3OH	(64)	49	$tGaH_3$	(73)	33	$\delta AlH\cdots H$	(74)
	τCH_3	(23)		δEHH	(35)		$\delta OH\cdots H$	(17)
				ν_2				
	τBH_3	(108)		$tGaH_3$	(48)		$tAlH_3$	(26)
70			52	$\delta GaH\cdots H$	(41)	42	tCH_3	(33)
							τCH_3OH	(24)
				ν_3				
82	τCH_3OH	(62)	65	τCH_3OH	(112)	60	τCH_3OH	(56)
	τCH_3	(37)					$tAlH_3$	(49)
				ν_4				
	$\delta BH...H$	(74)		τCH_3OH	(68)		τCH_3OH	(42)
122	$\delta OH...H$	(25)	88	$\delta GaH\cdots H$	(24)	92	$tAlH_3$	(33)
							tCH_3	(33)
				ν_5				
141	$\delta OH...H$	(49)	137	δOHH	(84)	142	$\delta OH\cdots H$	(29)
	$\delta BH...H$	(39)		δCOH	(15)		$\delta AlH\cdots H$	(57)
				ν_6				
296	$\boldsymbol{\nu_\sigma}$	**(102)**	**233**	$\boldsymbol{\nu_\sigma}$	**(81)**	**235**	$\boldsymbol{\nu_\sigma}$	**(81)**
				ν_7				
717	τOH^{bond}	(90)	671	τOH^{bond}	(61)	680	τOH^{bond}	(64)
				δGaH_3	(26)		δAlH_3	(25)

[a] ν, stretching; δ, deformation; τ, torsion; t, twisting.

TABLE 2: Calculated in Vacuum Harmonic and Anharmonic Frequencies of TFE in the Low-Frequency Range and their Assignment (PED, from B3LYP Calculations)[a]

	harmonic MP2 ν_{calc}, cm^{-1}	harmonic B3LYP ν_{calc}, cm^{-1}	anharmonic B3LYP ν_{calc}, cm^{-1}	assignment (PED)
1	131	113	112	$tCCH_2$ (98)
2	230	221	214	δCF_3 (39), δOCC (33)
3	326	315	292	τOH (41), δCF_3 (40)
4	395	382	356	τOH (47), δCF_3 (45)
5	427	414	404	δCF_3 (50)
6	540	526	521	δCF_3 (73)
7	554	537	532	δCF_3 (59)
8	672	655	648	νCF (21), δCF_3 (46), δOCC (16)

[a] ν, stretching; δ, deformation; τ, torsion; t, twisting.

TABLE 3: Calculated in Vacuum Harmonic and Anharmonic Frequencies of BH_4^-/TFE Dihydrogen Bonded Complex in the Low-Frequency Range and Their Assignment (PED, from B3LYP calculations)[a]

	harmonic MP2 ν_{calc}, cm^{-1}	harmonic B3LYP ν_{calc}, cm^{-1}	anharmonic B3LYP ν_{calc}, cm^{-1}	assignment (PED)
1	22	24	21	$tOCH_2$ (102)
2	56	63	61	$\delta OH\cdots H$ (25), tCF_3 (36), tBH_3 (51)
3	86	77	52	$\delta OH\cdots H$ (30), tBH_4 (76)
4	148	113	73	tBH_3 (100)
5	169	152	137	$\delta OH\cdots H$ (37), tBH_3 (21), $tCCH_2$ (39)
6	182	159	131	$\delta BH\cdots H$ (100)
7	250	235	223	$\delta BH\cdots H$ (10), δOCC (29), δCCF (30)
8	339	338	310	ν_σ (89)
9	361	349	345	δCF_3 (66)
10	431	419	412	δCF_3 (61)
11	538	524	519	δCF_3 (75)
12	555	538	533	δCF_3 (56)
13	664	647	638	νCF (23), δCF_3 (24), δCCF (25), δOCC (15)
14	693	705	667	τOH^{bond} (100)

[a] ν, stretching; δ, deformation; τ, torsion; t, twisting.

Increase of alcohol proton-donating ability in the DHB complexes with BH_4^- leads to high-frequency shift of ν_σ as one can see by comparing the Tables 1 and 3. Table 4, which collects all EH_4^- complexes with the two alcohols, exhibits the ν_σ frequency for TFE/EH_4^- in the range (281−339 cm^{-1}) higher than that of complexes with CH_3OH (233−295 cm^{-1}). The force constants (K_{HH}) of H···H mode change in parallel with the ν_σ frequencies. For example, K_{HH} for BH_4^-/ROH systems changes from 0.22 mdyn/Å for the DHB complex with CH_3OH to 0.35 mdyn/Å for that with TFE. Notably, that changing from CH_3OH to TFE decreases individuality of this vibration (from 81−102% to 63−81%). The frequency of this mode decreases in the order $BH_4^- > AlH_4^- \approx GaH_4^-$ for both proton donors in parallel with PED values.

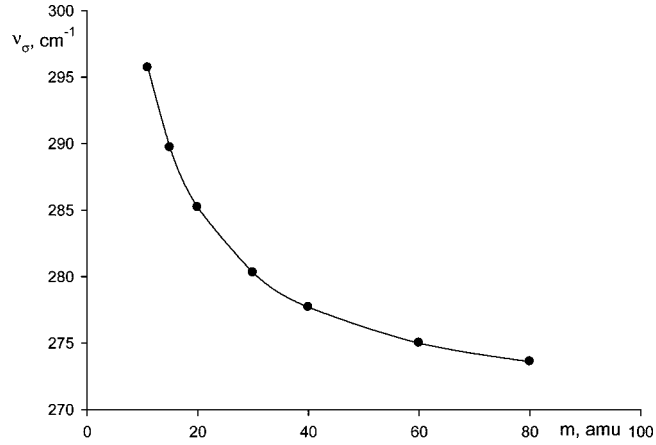

Figure 1. Dependence of ν_σ(HH) on the boron atom mass in the $H_3BH^-\cdots HOCH_3$ complex.

TABLE 4: Calculated MP2 and B3LYP Harmonic Frequencies of ν_σ(HH) Vibrations (in cm^{-1}), DHB Lengths (r(H···H), in Parentheses), and PED Impact (from B3LYP Calculations) of H···H Bond Stretch

	ROH = CH_3OH			ROH = CF_3CH_2OH		
hydride	MP2	B3LYP	PED	MP2	B3LYP	PED
BH_4^-	264 (1.723)	295 (1.654)	102	339 (1.580)	338 (1.553)	84
AlH_4^-	256 (1.632)	234 (1.622)	81	308 (1.512)	285 (1.513)	63
GaH_4^-	253 (1.666)	233 (1.628)	81	299 (1.531)	281 (1.520)	61

In order to elucidate the effect of the central-atom mass in the intermolecular H···H vibration, the calculation of the DHB complex $H_3BH^-\cdots HOCH_3$ was carried out by varying only one parameter, the boron mass (by using imaginary isotopes ^{20}B, ^{30}B, etc., Figure 1). The increase of the central atom mass from 11 to 80 a.m.u leads to the ν_σ frequency shift from 296 to 274 cm^{-1} ($\Delta\nu = 22$ cm^{-1}, Figure 1) and to some loss of specificity (PED changes from 102 to 91). Here, the maximal low shift was observed when increasing the mass from 11 (boron mass) to 27 (aluminum), whereas a much smaller shift was obtained when increasing the mass from 27 to 69 (gallium mass).

The tendency of ν_σ shifts due to the mass effect is correctly described with this simple model, although the values are underestimated in comparison with the actual frequency shift on changing boron by aluminum or gallium (see Table 4). The calculated shift on the mode ν_σ for the real complex $H_3{}^{69}GaH^-\cdots HOCH_3$ is 62 cm^{-1}, that is, nearly three times bigger than that obtained for the model $H_3{}^{70}BH^-\cdots HOCH_3$. This difference is probably connected with a difference in specificity of ν_σ mode between the model (^{70}B PED = 91%) and actual (^{69}Ga PED = 81%) systems.

We can qualitatively explain the dependence of the characteristic intermolecular H···H stretching mode on the central-atom mass by an increased mixing with other intramolecular modes. PED values notably decrease for Al and Ga hydrides (at ~20%). The same changes occur when we used more complex alcohol (TFE instead CH_3OH). Note that for several classic systems, decrease of intermolecular stretching vibrations (OH···Base) with increase of partner substituents mass were already reported.[41]

It is known that the value of the band shift due to the isotope substitution (for example, H/D, H/T) depends on the contribution of the hydrogen atom movement to the corresponding normal vibration. We carried out model calculations of the ν_σ frequency changes by increasing the mass of the hydrogen atom of EH_4^- or CH_3OH. The motion of the hydrogen atom of the tetrahydride

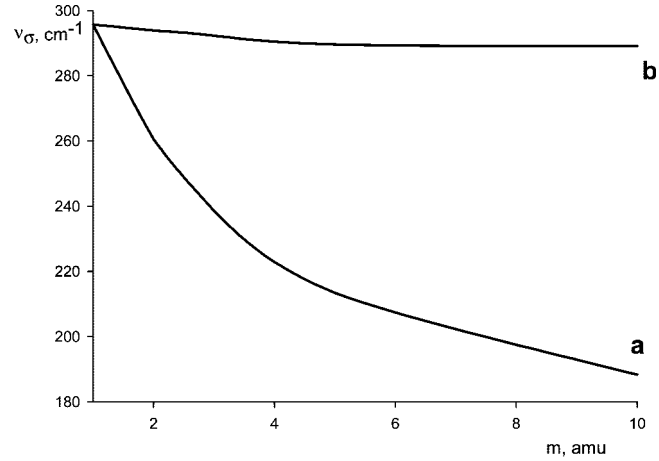

Figure 2. Dependence of ν_σ frequency in BH_4^-/CH_3OH complex on the mass of bonded H atom of hydride (a) and alcohol (b).

involved in the DHB makes the greatest contribution to the ν_σ mode; therefore, the increase of its atomic mass results in the largest frequency shifts (Figure 2). Conversely, the increase of the atomic mass of the protic hydrogen produces practically no change in the ν_σ frequency. The calculated frequency for the complex $CH_3OH\cdots DBD_3^-$ is 236 cm^{-1}, and the shift due to isotope effect is 40 cm^{-1}, with an isotope ratio H/D = 1.25, whereas for the complex with the stronger alcohol ($CF_3CH_2OH\cdots DBD_3^-$) νHD_{calc} = 279 cm^{-1}, and the isotope shift is larger (55 cm^{-1}, H/D ratio =1.20). Therefore, it is appropriate to use boron tetradeuteride BD_4^- and not ROD alcohol for the experimental study of isotope effect.

Therefore, beyond the dependence of the type of calculation (B3LYP or MP2) and the harmonic or anharmonic level of B3LYP, the values of ν_σ frequencies calculated for DHB complexes of B, Al, and Ga tetrahydrides with CH_3OH (Table 1) and BH_4^- with TFE (Tables 2, 3), as well as EH_4^- with both proton donors (Table 4), show that the hydride with minimal mass, namely, BH_4^-, and the alcohol with maximal proton donating ability (TFE) would be most suitable for the detailed experimental study,[25] because these factors both increase the frequency of the ν_σ vibration. Moreover, we could use some strong alcohols such as TFE only for a complex with BH_4^- because of the possibility of alcoholysis reactions in the case of GaH_4^- and AlH_4^-.[13,14]

3.2. IR Spectroscopic Investigation. On the basis of theoretical results, the DHB $H_3BH^-\cdots HOCH_2CF_3$ complex was chosen as the main system for the experimental study. Furthermore, this complex is stable at ambient temperature, thus allowing a thorough spectral investigation. The IR studies of the partners and DHB complexes of Bu_4NBH_4 were carried out also with fluorinated alcohols weaker (CFH_2CH_2OH) and stronger ($(CF_3)_2CHOH$) than TFE in low polar solvents (CH_2Cl_2 and $(CH_2Cl)_2$) targeted to find the intermolecular stretching vibrations (ν_σ) and to characterize the spectral properties of DHB formation in the low-frequency range.

In agreement with the calculations, no bands assigned to vibrations of Bu_4NBH_4 were found in the IR spectra in the range 300−600 cm^{-1}. Despite the fact that Bu_4N^+ cation must have vibrations in this range, their intensities are low and were not revealed in the spectra at the concentrations used. The IR spectrum of TFE measured in DCM is in rather good agreement with the calculated frequencies in the spectrum (B3LYP) in the same solvent (by using CPCM optimization in CH_2Cl_2, Table 5). The differences between the calculated and experimental

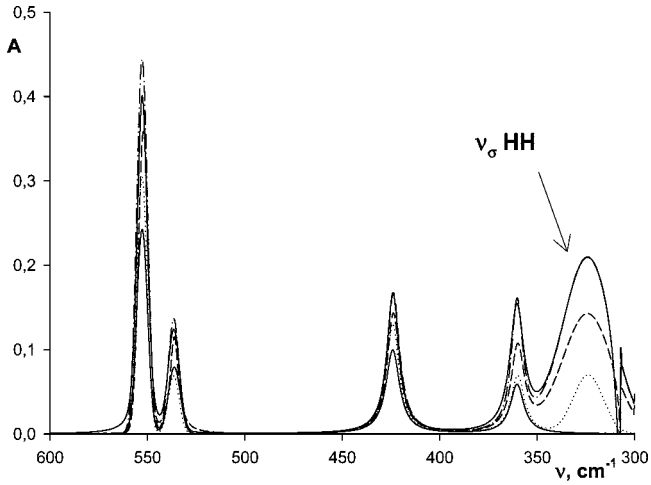

Figure 3. IR spectra of CF_3CH_2OH (0.08M) in presence of 0.4 M Bu_4NBH_4 at 210, 230, 250, and 270 K in CH_2Cl_2 solution.

TABLE 5: Experimental and B3LYP Calculated Frequencies of TFE in CH_2Cl_2 in the Low-Frequency Range

	ν_{exp} cm^{-1}	ν_{calc} cm^{-1}	assignment (PED)
1	552	536	δ CF_3 (59)
2	536	526	δ CF_3 (73)
3	420	411	δ CF_3 (50)
4	388	368	τ OH (47) δ CF_3 (45)
5	330	293	τ OH (41) δ CF_3 (40)

TABLE 6: Experimental Frequencies of TFE in Presence of Boron Tetrahydride Excess in CH_2Cl_2 and B3LYP Calculated Frequencies of TFE/BH_4^- Complex (with CPCM Optimization in CH_2Cl_2)

	ν_{exp} cm^{-1}	ν_{calc} cm^{-1}	assignment (PED)
1′	552	537	δ CF_3 (56)
2′	532	523	δ CF_3 (75)
3′	424	415	δ CF_3 (61)
4′	360	347	δ CF_3 (66)
5′	324	323	ν_σ (89)

frequencies for the three higher-frequency bands belonging to different deformations of CF_3 groups are 9−16 cm^{-1}. The next two bands assigned to the mixed torsion/deformation modes as in the Table 2 have larger deviations (20−37 cm^{-1}), although this change does not prevent the assignment of the experimental frequencies.

The addition of small excess of boron tetrahydride to the solution of TFE in CH_2Cl_2 (Figure 3) leads to very little shift of the three higher bands of TFE deformation ($\Delta\nu = 2-4$ cm^{-1}, bands 1−3, Table 6), whereas significant changes occur in the range 300−400 cm^{-1} as predicted by calculations (Table 3).

A narrow band at 360 cm^{-1} and a broadband at 324 cm^{-1} (Table 6) are observed instead of the two bands of TFE (388 and 330 cm^{-1}). The CPCM calculations indicate the same transformations of the modes during DHB formation as those determined in the gas phase (Tables 2, 3). The intermolecular stretching H···H vibration 323 cm^{-1} is similar to the experimental one ($\Delta\nu$ = 1 cm^{-1}). Thus, calculated frequencies in DCM agree with the experimental values better than those of the calculation in the gas phase; in vacuum, ν_σ are 339 and 338 cm^{-1} (by harmonic MP2 and B3LYP, respectively) and 310 cm^{-1} (anharmonic frequency by B3LYP). Note that PED value decrease from methanol to TFE as in the case of other computation (from 100 to 89%.).

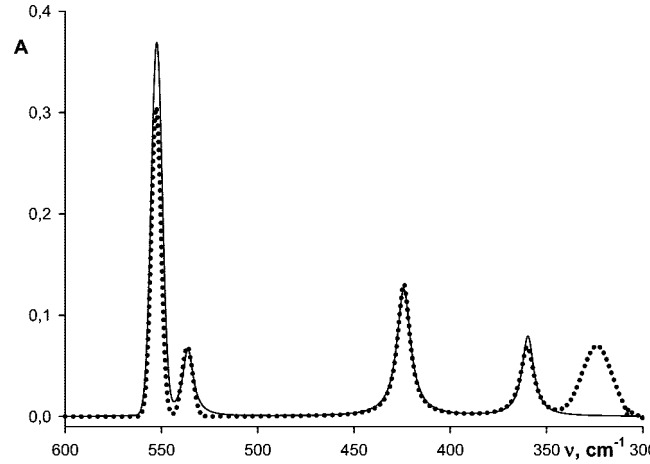

Figure 4. IR spectra of CF_3CH_2OH (0.08M) in presence of 0.4 M Bu_4NBH_4 (dashed) and 0.4 M Bu_4NBD_4 (solid) in CH_2Cl_2.

Therefore, the 4′ band at 360 cm^{-1} can be assigned to δ CF_3 (PED = 66%), and the last very broad band of DHB complex 5′ at 324 cm^{-1} can be assigned to the ν_σ stretching mode (Table 6). The agreement between the calculated and experimental values is good (for 1′−5′, differences are in the 1−15 cm^{-1} range). To find the additional evidence of such assignment, we studied the interaction with weaker (MFE) and stronger (HFIP), alcohols as well as the temperature dependence and isotope effect.

To study the temperature dependence, we carried out IR measurements in the interval of temperatures between 210−290 K. A right shift of the equilibrium (eq 1) upon cooling was obtained, showing favored DHB complex formation at low temperatures.

$$H_3BH^- + HOR \rightleftarrows H_3BH^- \cdots HOR \qquad (1)$$

The intensity of the broad band at 324 cm^{-1} increases on cooling, confirming the assignment to the ν_σ mode. Intensities of the other bands in the 300−600 cm^{-1} range change less, and changes are in line with usual band temperature dependence of free TFE (Figure 3).

Isotope substitution of Bu_4NBH_4 by Bu_4NBD_4 results in the ν_σ band disappearance. The intensity and position of the other bands in this region remain unchanged (Figure 4). The theoretically calculated isotope ratio ν_H/ν_D for the complex $CF_3CH_2OH\cdots{}^-HBH_3$ is 1.2, and therefore, the ν(HD) band in the IR spectra of $CF_3CH_2OH\cdots{}^-DBD_3$ complex should be somewhere between 270 cm^{-1} ($\nu(HD)_{exp}/\nu(HH)_{exp}$ = 1.2) and 279 cm^{-1} ($\nu(HD)_{calc}$). Unfortunately, the solvent (CH_2Cl_2 or $(CH_2Cl)_2$) has a broadband at 285 cm^{-1}, which masks any band in the range 260−300 cm^{-1}. The use of other solvents (e.g, hexane) is precluded by the low solubility of Bu_4NBH_4.

Interaction of BH_4^- with a weaker proton donor (MFE) reveals spectral trends similar to those with TFE. The band assigned to ν_σ appears at a frequency (318 cm^{-1}) lower than that for TFE as was expected from calculations. According to the theoretical calculations, interaction with stronger proton donor should shift ν_σ to a higher range. Thus, the ν_σ band of the DHB complex with HFIP appears at 362 cm^{-1}, being 44 and 38 cm^{-1} higher than that in the complexes with MFE and TFE, respectively. Notably, this band can be observed only at low temperature (210−230 K, Figure 5). At 230 K, the intensity of the H···H stretch decreases, disappearing with further warming. The cause of such changes is dihydrogen evolution

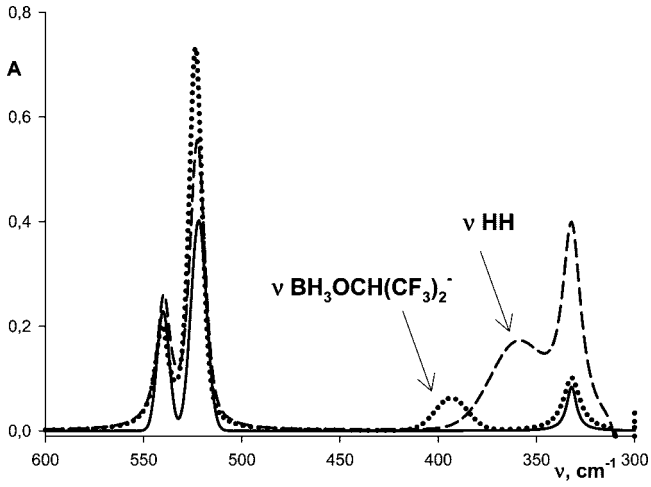

Figure 5. IR spectra of $(CF_3)_2CHOH$ (0.08M, solid line) and in presence of Bu_4NBH_4 (0.4M) at 210 K (dashed line) and 250 K (dotted line) in CH_2Cl_2.

TABLE 7: Spectral ($\Delta\nu$OH, ν_σ), Thermodynamic ($-\Delta H_{exp}$), and Structural (rH···H) Parameters of DHB Complexes of Boron Tetrahydride with Different Proton Donors

ROH	ν_σ, cm^{-1}, in CH_2Cl_2	$\Delta\nu$OH	$-\Delta H_{exp}$, kcal/mol, in CH_2Cl_2[a]	rH···H, Å
CFH_2CH_2OH	318	247	4.6	1.63
CF_3CH_2OH	324	290	5.2	1.55
$(CF_3)_2CHOH$	362	402	6.5	1.46

[a] Data from refs 11 and 13.

and formation of alkoxoboron complex (equilibrium in eq 2). The equilibrium (eq 2) shifts to the reaction product.

$$H_3BH^- + HOR \rightleftarrows H_3BH^- \cdots HOR \rightarrow H_3BOR^- + H_2 \quad (2)$$

A new band at 394 cm^{-1} appears in the IR spectra at 250 K and grows with the temperature increase. This new band is assigned to the organyloxy derivative of tetrahydride formed in the reaction between BH_4^- with HFIP at the 250−290 K range (eq 2). Calculations showed the strongly mixed mode of this vibration including δCF_3 (66%), νBO (12%), νCO (12%), and δCO (9%) impacts in PED.

We are interested in the relations between the frequency and the structure, as well as the strength of the complexes. To analyze such relations, we compare the data in the high- and low-frequency ranges by considering the changes of OH stretching vibrations for complexes of BH_4^- with CH_3OH, TFE, and HFIP, spectral parameters of ν_σ, strength of DHB, and H···H distance (Table 7).

Table 7 collects the data of ν_σ band positions measured now together with the $\Delta\nu$OH, enthalpy ($-\Delta H_{exp}$), and H···H distances which have been determined in our previous works.[11,13,14] One can see that the ν_σ frequency increases with proton-donor ability of alcohols in parallel with low-frequency shifts of νOH, strength of the complexes ($-\Delta$H), and decrease of H···H distances. Therefore, we can conclude that the correlation between the parameters of high- and low-frequency ranges, the thermodynamic, and the structural characteristics of DHB complexes take place.

4. Conclusions

The computational investigation by normal coordinate analysis of the low-frequency range IR spectra of DHB complexes between the EH_4^- hydrides and two proton donors (CH_3OH, TFE) was initially carried out. Different approaches were followed for the frequency calculations: in vacuum harmonic (MP2 and B3LYP), in vacuum anharmonic (B3LYP), and in DCM (B3LYP). The interpretation of the low-frequency vibrations on the basis of calculated PED values allows us to assign six new vibrations in DHB complexes in comparison with those of the partners. All of them are strongly mixed (δ and τ), except the intermolecular H···H stretching mode (ν_σ) which has high characteristic individual PED in the range 81−100%. The relation between the frequency of the H···H stretching mode and the proton donor strength and between the central-element mass and isotope substitution (ν_H/ν_D) in the hydride complexes was established. These computational results guided the choice of the most convenient system for the subsequent experimental study. Such system involves the lightest hydride (BH_4^-) and rather strong proton donor (TFE). The experimental measurements were made also with the weaker (MFE) and stronger (HFIP) proton donors. This investigation confirmed the calculated assignment of ν_σ and the influence of the alcohol strength. The study of temperature dependence of the IR spectra showed that the intensity of the broad ν_σ band increases with cooling because of the equilibrium shift to the DHB formation. In the case of the strongest proton donor, HFIP, proton transfer and dihydrogen evolution occur above 250 K. The ν_σ band disappears, and the band of the alkoxy product appears and increases at warming. The isotope effect, temperature dependence, and influence of the proton-donor strength observed experimentally were in agreement with DFT calculation results. In conclusion, the intermolecular stretching mode characterizing intrinsic DHB vibrations was determined for the first time by combining experimental and theoretical approaches.

Acknowledgment. This work was supported by the Russian Foundation for Basic Research (no. 07-03-00739) and Spanish MEC (Project no. CTQ2005-09000-CO2-01). O.A.F. thanks INTAS YSF (06-1000014-5809). A.L. thanks the Generalitat de Catalunya for a Distinció per a la Promoció de la Recerca Universitària. The use of computational facilities of the Centre de Supercomputació de Catalunya (CESCA) is gratefully appreciated.

Supporting Information Available: Tables of optimized geometries (Cartesian coordinates) for the calculated species. This material is available free of charge via the Internet at http://pubs.acs.org.

References and Notes

(1) Crabtree, R. H.; Siegbahn, P. E. M.; Eisenstein, O.; Rheingold, A. L.; Koetzle, T. F. *Acc. Chem. Res.* **1996**, *29*, 348.

(2) Shubina, E. S.; Belkova, N. V.; Epstein, L. M. *J. Organomet. Chem.* **1997**, *17*, 536–537.

(3) Epstein, L. M.; Shubina, E. S. *Coord. Chem. Rev.* **2002**, *231*, 165.

(4) Belkova, N. V.; Shubina, E. S.; Epstein, L. M. *Acc. Chem. Res.* **2005**, *38*, 624.

(5) Alkorta, I.; Rozas, I.; Elguero, J. *Chem. Soc. Rev.* **1998**, *27*, 163.

(6) Coustelcean, R.; Jackson, J. E. *Chem. Rev.* **2001**, *101*, 1963.

(7) Giner Planas, J.; Viñas, C.; Teixidor, F.; Comas-Vives, A.; Ujaque, G.; Lledós, A.; Light, M. E.; Hursthouse, M. B. *J. Am. Chem. Soc.* **2005**, *127*, 15976.

(8) Belkova, N. V.; Besora, M.; Epstein, L. M.; Lledós, A.; Maseras, F.; Shubina, E. S. *J. Am. Chem. Soc.* **2003**, *125*, 7715.

(9) Yao, W.; Eisenstein, O.; Crabtree, R. H. *Inorg. Chim. Acta* **1997**, *254*, 105.

(10) Crabtree, R. H. *J. Organomet. Chem.* **1998**, *557*, 111.

(11) Epstein, L. M.; Shubina, E. S.; Bakhmutova, E. V.; Saitkulova, L. N.; Bakhmutov, V. I.; Gambaryan, N. P.; Chistyakov, A. L.; Stankevich, I. V. *Inorg. Chem.* **1998**, *37*, 3013.

(12) Shubina, E. S.; Bakhmutova, E. V.; Filin, A. M.; Sivaev, I. B.; Teplitskaya, L. N.; Chistyakov, A. L.; Stankevich, I. V.; Bakhmutov, V. I.; Bregadze, V. I.; Epstein, L. M. *J. Organomet. Chem.* **2002**, *657*, 155.

(13) Belkova, N. V.; Filippov, O. A.; Filin, A. M.; Teplitskaya, L. N.; Shmyrova, Y. V.; Gavrilenko, V. V.; Golubinskaya, L. M.; Bregadze, V. I.; Epstein, L. M.; Shubina, E. S. *Eur. J. Inorg. Chem.* **2004**, 3453.

(14) Filippov, O. A.; Filin, A. M.; Tsupreva, V. N.; Belkova, N. V.; Lledos, A.; Ujaque, G.; Epstein, L. M.; Shubina, E. S. *Inorg. Chem.* **2006**, *45*, 3086.

(15) Custelcean, R.; Vlassa, M.; Jackson, J. E. *Angew. Chem.* **2000**, *112*, 3437. Custelcean, R.; Vlassa, M.; Jackson, J. E. *Angew. Chem., Int. Ed.* **2000**, *39*, 3299.

(16) Custelcean, R.; Jackson, J. E. *J. Am. Chem. Soc.* **2000**, *122*, 5251.

(17) Custelcean, R.; Jackson, J. E. *J. Am. Chem. Soc.* **1998**, *120*, 12935.

(18) Custelcean, R.; Jackson, J. E. *Angew. Chem.* **1999**, *111*, 1748. Custelcean, R.; Jackson, J. E. *Angew. Chem., Int. Ed.* **1999**, *38*, 1661.

(19) Hwang, J. W.; Campbell, J. P.; Kozubowski, J.; Hanson, S. A.; Evans, J. F.; Gladfelter, W. L. *Chem. Mater.* **1995**, *7*, 517.

(20) Klooster, W. T.; Koetzle, T. F.; Siegbahn, P. E. M.; Richardson, T. B.; Crabtree, R. H. *J. Am. Chem. Soc.* **1999**, *121*, 6337.

(21) Orlova, G.; Scheiner, S. *J. Phys. Chem. A* **1998**, *102*, 260.

(22) Orlova, G.; Scheiner, S. *J. Phys. Chem. A* **1998**, *102*, 4813.

(23) Cramer, C. J.; Gladfelter, W. L. *Inorg. Chem.* **1997**, *36*, 5358.

(24) Kar, T.; Scheiner, S. *J. Chem. Phys.* **2003**, *119*, 1473.

(25) Alkorta, I.; Elguero, J.; Mo, O.; Vanez, M.; Del Bene, J. *J. Phys. Chem. A* **2002**, *106*, 9325.

(26) Grabowski, S. J.; Sokalski, W. A.; Leszczynski, J. *J. Phys. Chem. A* **2004**, *108*, 5823.

(27) Grabowski, S. J.; Sokalski, W. A.; Leszczynski, J. *J. Phys. Chem. A* **2005**, *109*, 4331.

(28) McDowel, S.; Forde, T. S. *J. Mol. Struct. (Theochem)* **2003**, *624*, 109.

(29) Hugas, D.; Simon, S.; Duran, M. *Struct. Chem.* **2005**, *16*, 257.

(30) Solimannejad, M.; Scheiner, S. *J. Phys. Chem. A* **2005**, *109*, 11933.

(31) Solimannejad, M.; Boutalib, A. *Chem. Phys.* **2006**, *320*, 275.

(32) Frisch, M. J.; Trucks, G. W.; Schlegel, H. B.; Scuseria, G. E.; Robb, M. A.; Cheeseman, J. R.; Montgomery, J. A., Jr.; Vreven, T.; Kudin, K. N.; Burant, J. C.; Millam, J. M.; Iyengar, S. S.; Tomasi, J.; Barone, V.; Mennucci, B.; Cossi, M.; Scalmani, G.; Rega, N.; Petersson, G. A.; Nakatsuji, H.; Hada, M.; Ehara, M.; Toyota, K.; Fukuda, R.; Hasegawa, J.; Ishida, M.; Nakajima, T.; Honda, Y.; Kitao, O.; Nakai, H.; Klene, M.; Li, X.; Knox, J. E.; Hratchian, H. P.; Cross, J. B.; Bakken, V.; Adamo, C.; Jaramillo, J.; Gomperts, R.; Stratmann, R. E.; Yazyev, O.; Austin, A. J.; Cammi, R.; Pomelli, C.; Ochterski, J. W.; Ayala, P. Y.; Morokuma, K.; Voth, G. A.; Salvador, P.; Dannenberg, J. J.; Zakrzewski, V. G.; Dapprich, S.; Daniels, A. D.; Strain, M. C.; Farkas, O.; Malick, D. K.; Rabuck, A. D.; Raghavachari, K.; Foresman, J. B.; Ortiz, J. V.; Cui, Q.; Baboul, A. G.; Clifford, S.; Cioslowski, J.; Stefanov, B. B.; Liu, G.; Liashenko, A.; Piskorz, P.; Komaromi, I.; Martin, R. L.; Fox, D. J.; Keith, T.; Al-Laham, M. A.; Peng, C. Y.; Nanayakkara, A.; Challacombe, M.; Gill, P. M. W.; Johnson, B.; Chen, W.; Wong, M. W.; Gonzalez, C.; Pople, J. A. *Gaussian 03*, revision C.02; Gaussian, Inc.: Wallingford, CT, 2004.

(33) Becke, A. D. *J. Chem. Phys.* **1993**, *98*, 5648.

(34) Moller, C.; Plesset, M. S. *Phys. Rev.* **1934**, *46*, 618–622.

(35) Barone, V.; Cossi, M. *J. Phys. Chem. A* **1998**, *102*, 1995.

(36) Barone, V. *J. Chem. Phys.* **2004**, *120*, 3059.

(37) Barone, V. *J. Chem. Phys.* **2005**, *122*, 014108.

(38) Yagola, A. G.; Kochikov, I. V.; Kuramshina, G. M.; Pentin, Y. A. *Inverse Problems of Vibrational Spectroscopy*; VSP: Utrecht, 1999.

(39) Scott, A. P.; Radom, L. *J. Phys. Chem.* **1996**, *100*, 16502.

(40) Merrick, J. P.; Moran, D.; Radom, L. *J. Phys. Chem. A* **2007**, *111*, 11683.

(41) Knozinger, E.; Schrems, O. In *Vibrational Spectra and Structures, A Series of Advances*; Durig, J. R., Ed.; Elsevier: Amsterdam, 1987; Vol. 16, p 142.

JP804303J